Epitaxial Chemical Vapor Deposition Growth of Single-Layer Graphene over Cobalt Film Crystallized on Sapphire

Hiroki Ago,[†,‡,*] Yoshito Ito,[‡] Noriaki Mizuta,[‡] Kazuma Yoshida,[‡] Baoshan Hu,[†] Carlo M. Orofeo,[†] Masaharu Tsuji,[†,‡] Ken-ichi Ikeda,[‡] and Seigi Mizuno[‡]

[†]Institute for Materials Chemistry and Engineering, Kyushu University, Kasuga, Fukuoka 816-8580, Japan, and [‡]Graduate School of Engineering Sciences, Kyushu University, Kasuga, Fukuoka 816-8580, Japan

ABSTRACT Epitaxial chemical vapor deposition (CVD) growth of uniform single-layer graphene is demonstrated over Co film crystallized on c-plane sapphire. The single crystalline Co film is realized on the sapphire substrate by optimized high-temperature sputtering and successive H_2 annealing. This crystalline Co film enables the formation of uniform single-layer graphene, while a polycrystalline Co film deposited on a SiO_2/Si substrate gives a number of graphene flakes with various thicknesses. Moreover, an epitaxial relationship between the as-grown graphene and Co lattice is observed when synthesis occurs at 1000 °C; the direction of the hexagonal lattice of the single-layer graphene completely matches with that of the underneath Co/sapphire substrate. The orientation of graphene depends on the growth temperature and, at 900 °C, the graphene lattice is rotated at 22 ± 8° with respect to the Co lattice direction. Our work expands a possibility of synthesizing single-layer graphene over various metal catalysts. Moreover, our CVD growth gives a graphene film with predefined orientation, and thus can be applied to graphene engineering, such as cutting along a specific crystallographic direction, for future electronics applications.

KEYWORDS: graphene · epitaxy · crystal orientation · CVD · growth mechanism

Graphene, a monolayer of carbon atoms arranged into a hexagonal lattice, has attracted a great interest because of their unique structure and promising properties.[1] In particular, extraordinary high carrier mobilities, chemical stability, and a two-dimensional structure that is applicable to top-down lithography promise applications in future electronic devices such as touch panels, high frequency transistors, solar cells, and logic circuits.[2−5] Exfoliated graphene has been widely used because highly crystalline graphene, obtained by simply a transfer from graphite using scotch tape, lacks uniformity in thickness and size.[1] For practical applications, making high-quality, large-area graphene with homogeneous thickness is demanded. Thermal decomposition of SiC and vacuum pyrolysis over transition metal crystals, such as Ru(0001), Ir(111), Ni(111), offer well-defined single- and/or few-layer graphene films.[6−12] However, these single crystalline substrates are very expensive and their available size is limited.

Recently, catalytic chemical vapor deposition (CVD) has been applied to grow large-area graphene at low cost.[13−17] Ni film deposited on a SiO_2/Si wafer has been widely investigated for the CVD growth, but the graphene suffers from inhomogeneous film thickness which varies from single to multilayers.[13−16] Being different from a Ni film, a Cu film was reported to catalyze the growth of single-layer graphene selectively.[17] This catalytic effect of Cu is explained by the self-limiting mechanism due to very low carbon solubility in Cu (~0.03 atom % at 1000 °C[18]).[17] On the other hand, because Ni has much higher carbon solubility at high temperature (~1 atom %[18]), it is believed that multilayer graphene formation is inevitable; but the graphene precipitation occurs *via* bulk diffusion of carbon atoms in a Ni film so that control of the number of layers is quite difficult.[19]

All the CVD syntheses reported so far utilized polycrystalline metal films, including Ni and Cu films, as the catalyst. Reflecting this polycrystalline nature of the catalyst, as-synthesized graphene films have many domain boundaries, and, importantly, the orientation of the hexagonal lattice has not been addressed for the CVD-grown graphene so far.

Here, we present the formation of a crystalline Co film on a sapphire c-plane substrate and successive growth of uniform and orientation-controlled single-layer graphene over the Co film. The single crystalline Co film is obtained by high temperature sputtering and H_2 annealing. Although Co has high carbon solubility (~1 atom % at 1000 °C[18]) similar to Ni, single-layer graphene selectively grows on our crystalline Co film. Our result shows that the

*Address correspondence to ago@cm.kyushu-u.ac.jp.

Received for review September 24, 2010 and accepted November 15, 2010.

Published online November 24, 2010. 10.1021/nn102519b

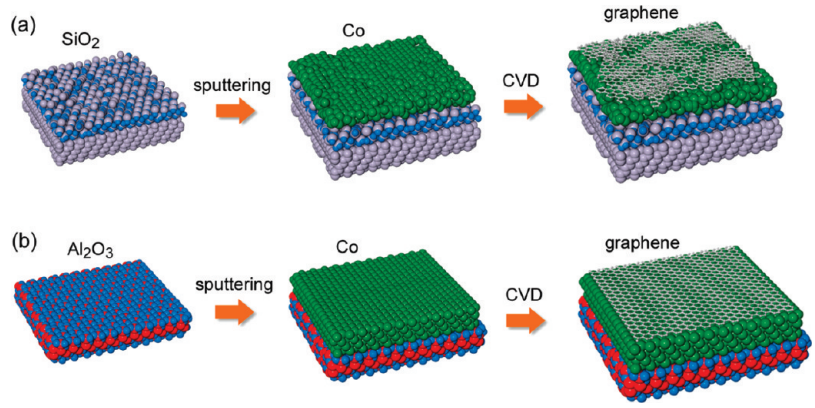

Figure 1. Schematics of the CVD growth of graphene over Co films deposited on SiO_2/Si (a) and sapphire c-plane (b) substrates. (a) Polycrystalline Co film is formed on the SiO_2 surface, which gives disordered graphene with broad layer distribution and randomly orientated small domains. (b) On the other hand, crystalline Co film is formed on sapphire c-plane and assists the growth of uniform, well-defined graphene with controlled orientation.

crystallinity of the metal catalyst determines the homogeneity of the graphene film. Furthermore, when we synthesize graphene at 1000 °C, the graphene orientation completely matches that of the underneath Co lattice, indicating epitaxial graphene growth under atmospheric CVD. Mis-orientation of graphene against the Co lattice with a rotation angle of 22 $\pm$ 8° is observed when the graphene is grown at 900 °C.

RESULTS AND DISCUSSION

Figure 1 illustrates our approach of the epitaxial CVD growth of graphene over a crystalline Co film. In the traditional CVD experiment (Figure 1a), a metal film is deposited on a Si wafer with an oxide layer at the top (SiO_2/Si substrate). Reflecting the amorphous nature of the surface SiO_2 layer, the metal film has a polycrystalline structure that contains a number of grain boundaries. Graphene formed on this polycrystalline metal consists of many small domains with different layer numbers, which might deteriorate the intrinsic properties of ideal graphene. As graphene has a tendency to precipitate from the grain boundaries of a metal catalyst film, the presence of many grain boundaries gives uncontrollable precipitation of graphene.[19] Alternatively, as illustrated in Figure 1b, we prepare a highly crystalline metal film by deposition on a single crystal substrate. In this work, we used c-plane sapphire as a substrate, because large sapphire wafers are available with relatively low cost owing to the demands from the light emitting diode (LED) industry, and crystal films, such as Cu and Ag, are obtained on the sapphire c-plane due to matching of the symmetry and little lattice mismatch.[20] Sapphire's thermal and chemical stability is also suitable for CVD growth. A uniform graphene film is epitaxially grown by atmospheric CVD on this crystalline Co film. We previously reported that few-layer graphene is preferentially formed inside triangular- and square-shaped pits when thin Co film (50 nm) and polystyrene are used as catalyst and carbon precursor, respectively,[21] but no large-area homogeneous graphene films were obtained.

Graphene films were synthesized by atmospheric CVD with a mixed flow of CH_4 and H_2 gases mainly at 1000 °C. The substrate was quenched after the reaction by rapid removal from the furnace.[13,14,22] The reaction scheme is displayed in the Supporting Information (Figure SI-1). For comparison, the CVD at 900 °C was also performed. The Co film and as-grown graphene were investigated by X-ray diffraction (XRD), optical microscope, and scanning electron microscope (SEM) measurements, as shown in Figure 2. First, we studied effects of the sputtering temperature and annealing condition. When the Co was sputtered onto c-plane sapphire at room temperature (RT), two diffraction peaks were observed after the CVD at 1000 °C (Figure 2a). The peak at 52° is assigned to Co face-centered cubic (fcc) (002) diffraction, and the peak at 44° is assigned to either hexagonal close-packed (hcp) Co(0002) or fcc(111). The presence of two peaks indicates the polycrystalline nature of the Co film even after the CVD at a high temperature of 1000 °C. Moreover, the microscope images show very rough Co morphology (Figure 2e), indicating deterioration of the Co film probably due to heat-induced melting and deformation.

When a Co film was sputtered onto a sapphire substrate which is heated at 500 °C, the Co fcc(002) diffraction peak disappeared while the Co hcp(0002) (or Co fcc(111)) peak remained (Figure 2b). This suggests improvement of the crystallinity of the Co film. In the high-temperature sputtering, Co atoms can easily migrate due to excess energy supplied from the heated substrate and form more ordered crystalline structure. It is known that the transition of bulk Co occurs from the hcp structure to the high-temperature stable fcc structure at a temperature of ~415 °C.[23] Considering the rapid quenching after CVD, Co fcc(111) substrate is likely to be preserved, but an electron backscatter electron diffraction (EBSD) analysis suggested the formation of hcp(0001) surface, as will be shown later. We

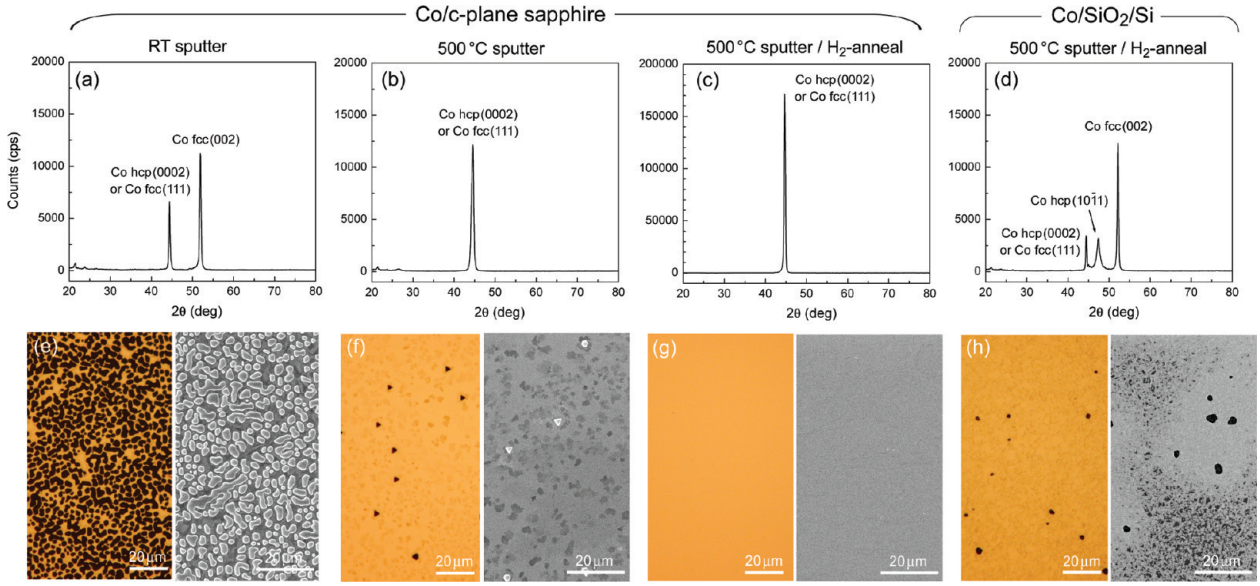

Figure 2. (a−d) XRD profiles of the Co films measured after CVD at 1000 °C. (e−h) Optical microscope (left) and SEM (right) images of the metal surfaces obtained after the CVD. (a,e) Co film was sputtered at room temperature on c-plane sapphire and subjected to the CVD. (b,f) Co film was sputtered at 500 °C on c-plane sapphire and subjected to CVD. (c,g) Co film was sputtered at 500 °C on c-plane sapphire, annealed at 500 °C in H_2/Ar flow for 3 h, and then subjected to CVD. (d,h) SiO_2/Si substrate was used instead of sapphire with other experimental conditions identical to those in panels c,g.

note that both hcp(0001) and fcc(111) structures have the same surface atomic arrangement with closest packing geometry. The degree of crystallization of the 500 °C-sputtered Co film is still not high enough, because the intensity and width of the Co hcp(0002) (or Co fcc(111)) peak are similar to those of the RT-sputtered Co film (see Figure 2a,b). As seen from Figure 2f, the Co film became smoother by sputtering at the high temperature, but small triangular pits were seen by an optical microscope. The same orientation of these pits suggests the crystalline nature of the Co film. One can see relatively thick graphene flakes with several μm sizes on the Co surface. These graphene flakes correspond to the light brown and dark gray areas in the optical microscope and SEM images, respectively. Note that these flakes have various contrasts, signifying a broad distribution in the number of graphene layers.

We have thoroughly studied postdeposition treatment to achieve a more uniform graphene film and found that heat treatment in H_2/Ar flow at the moderate temperature can improve the crystallinity of the Co film. The optimized H_2 annealing temperature and period were 500 °C and 3 h, respectively. Although some groups used H_2 annealing at the temperature used for CVD (900−1000 °C),[13,14] we found that the moderate temperature (500 °C) is more suitable for our sputtered Co films on sapphire; the H_2 annealing at the CVD temperature deteriorated the quality of the Co film, making the surface rougher. The H_2 annealing at 500 °C greatly improved the crystallinity of the Co film, as seen from the stronger diffraction peak and narrower peak width compared with the nonannealed sample (see Figure 2b,c). This result verifies the formation of highly crystalline Co film on c-plane sapphire after the appropriate processes. Reflecting the highly crystalline nature, the Co film shows continuous and smooth surface with no pits. Moreover, no thick graphene flakes were seen by the optical microscope and SEM images (Figure 2g), which is quite different from other samples. As we will discuss later, the uniform contrast represents the formation of uniform single-layer graphene on the Co film. The atomic force microscope (AFM) image also showed the smoothest surface (see Supporting Information, Figure SI-2c).

For comparison, we studied the crystallinity of a Co film that is deposited on the SiO_2/Si wafer at 500 °C. Even after the H_2 annealing, multiple diffraction peaks were obtained by the XRD (Figure 2d) with a new peak corresponding to a Co hcp(10$\bar{1}$1) phase. This result highlights the polycrystalline nature of the Co film. Microscope images shown in Figure 2h indicate the formation of thick graphene flakes together with irregular-shaped pits. The irregular-shape of the pits also supports the polycrystalline Co structure.

Crystalline orientation and grain size of Co films were further investigated with (EBSD). Supporting Information, Figure SI-3 indicates the orientation distributions of Co films deposited on c-plane sapphire and SiO_2/Si. The Co film on sapphire is suggested to have an hcp(0001) plane normal to the surface. Importantly, no clear grain boundaries were observed in the inspected area (80 μm × 200 μm), signifying the formation of the single crystalline Co film. On the other hand, the Co on SiO_2/Si mainly has a fcc(001) surface with a large number of grain boundaries and it shows various in-plane orientations. It is apparent that the Co on SiO_2/Si is polycrystalline with a grain size of less than 3

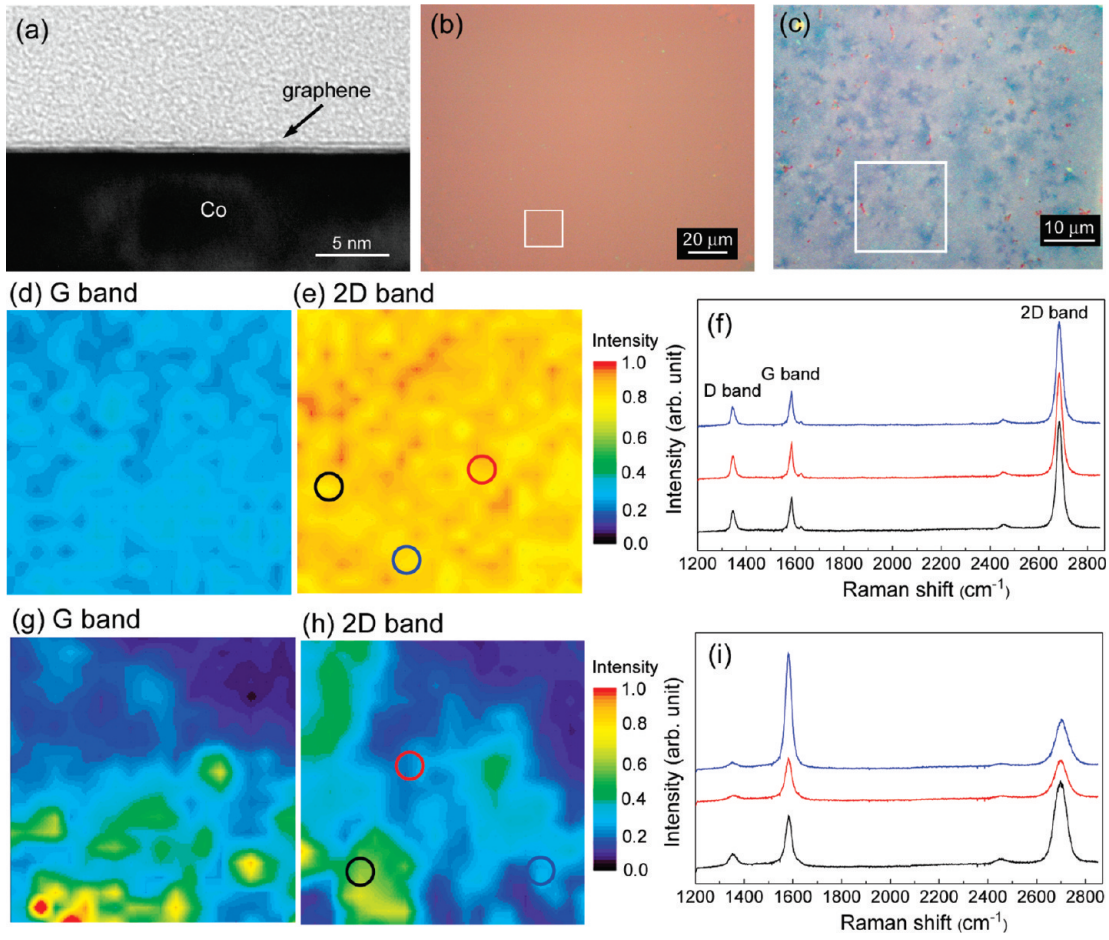

Figure 3. (a) Cross-sectional TEM image of single-layer graphene grown on the crystalline Co film. Optical microscope images of transferred graphene films from graphene/Co/sapphire (b) and graphene/Co/SiO_2 (c) onto target SiO_2(300 nm)/Si substrates. Raman mapping images of G band (1585 cm^{-1}) (d) and 2D band (2685 cm^{-1}) (e) intensities measured for the graphene transferred from Co/sapphire substrate. The mapping area is indicated by a white square in panel b. (f) The corresponding Raman spectra marked in panel e. (g−i) Raman mapping images and spectra of the graphene transferred from the Co/SiO_2 substrate. The peak intensities at 1585 and 2700 cm^{-1} are plotted in panels g and h, respectively, and the spectra (i) are measured at the positions shown in panel h. The mapping area is indicated by a white square in panel c.

μm. These results are consistent with the XRD profiles shown in Figure 2.

We also found that the crystallinity of a Co film is dependent on the crystal plane of sapphire substrates. On a- and r-plane sapphire substrates, the Co films have polycrystalline structure and consequently gave thick graphene flakes, as depicted in Supporting Information (Figure SI-4). Only c-plane sapphire gave crystalline Co film and uniform graphene. Therefore, we conclude that a substrate greatly influences the crystallinity of the catalyst metal film and that symmetry of the substrate is essential for the crystallization of the film.

Shown in Figure 3a is the cross-sectional transmission electron microscope (TEM) image of the graphene/Co/c-plane sapphire. The specimen was directly cut from the substrate surface using focused ion beam (FIB). One can see that single-layer graphene is present on the Co surface. For wide area inspection, the graphene film was transferred onto a target SiO_2(300 nm)/Si substrate. Figure 3b,c shows optical microscope images of the graphene films transferred from the Co films deposited on c-plane sapphire and SiO_2/Si substrates (both samples were sputtered at 500 °C and subjected to the H_2 annealing). The graphene transferred from the Co/c-plane sapphire showed uniform color contrast which can be assigned to single-layer graphene based on Raman and optical measurements, as will be described later. On the other hand, the graphene transferred from Co/SiO_2/Si (Figure 3c) showed a wide color contrast, suggesting the formation of multilayer graphene flakes together with single-layer graphene. These results are consistent with the micrographs taken before the transfer (see Figure 2g,h). It is noted that the image of the transferred graphene from Co/SiO_2/Si (Figure 3c) resembles that in previous literatures of the typical CVD-grown graphene over Ni films deposited on SiO_2/Si.[13−16]

Raman mapping measurements were performed for the transferred graphene films. Figure 3d,e shows intensities of the G and 2D bands measured for a 19 μm × 19 μm area. The relative intensity of 2D band to G band (I_{2D}/I_G) is one indication of layer numbers; when

the I_{2D}/I_G value is ~3, ~1, and less than 1, the number of layers are one, two, and more than two, respectively.[14,17] The Raman mapping images and corresponding spectra of the graphene grown on the Co/c-plane sapphire (Figure 3d−f) prove that the whole measured area solely consists of single-layer graphene, because the whole area shows the I_{2D}/I_G ratio of ~3. The G and 2D bands are observed at ~1585 and ~2675 cm^{-1}, respectively. Moreover, the 2D band is narrow (the full width at half-maximum (fwhm) is 30−40 cm^{-1}) and can be fitted with a single Lorentzian, supporting the growth of uniform single-layer graphene. We noticed that the SEM contrast before the transfer is closely resembles the optical microscope image taken after the transfer; thus, the uniformity of a graphene film can be assessed for the as-grown graphene by SEM measurement when the metal surface is smooth enough. We observed that the single-layer graphene extends more than 1 mm^2 from the SEM image, but in some areas of a 10 mm ×10 mm substrate multilayer graphene formation was observed. For the graphene grown on the Co/SiO_2/Si substrate, the I_{2D}/I_G showed wide variation from 0.3−3 depending on the position (see Figure 3g−i). This represents the formation of inhomogeneous graphene films with different layer numbers including multilayer graphene with >5 layers. It is seen that the multilayer graphene has weaker D bands (Figure 3i, blue and red lines) than single-layer graphene (black line). The first graphene layer attached to the Co surface is likely to show stronger D band than other upper layers. This is because the first layer is mostly affected by the lattice strain during growth and also by the etching process which dissolves the underneath Co film.

The D band originated in defects or disordered carbon is relatively strong for our epitaxial graphene formed on the crystalline Co (Figure 3f). We measured the Raman spectrum of as-grown graphene before transfer, as shown in Supporting Information, Figure SI-5. The relative intensity of D band to G band (I_D/I_G) was much smaller than that measured after the transfer, which signifies the possibility of graphene damage during transfer. The etching solution may damage the graphene film, but there can be other factors; our etching solution (1 M $FeCl_3$ aqueous solution) is used to transfer CVD graphene with a little less damage to graphene.[16] In the case of the Co catalyst film, the formation of a Co−C (graphene) covalent bond is possible, considering the higher binding energy calculated for the graphene−Co(111) interface than that for the graphene−Cu(111).[24] The dissolution of the Co film may give dangling bonds in the graphene sheet, which reduces the domain size of the graphene and increases the D band intensity. Further study is necessary for the understanding of the interface interaction between graphene and the crystalline Co film and also for reduction of the D band intensity.

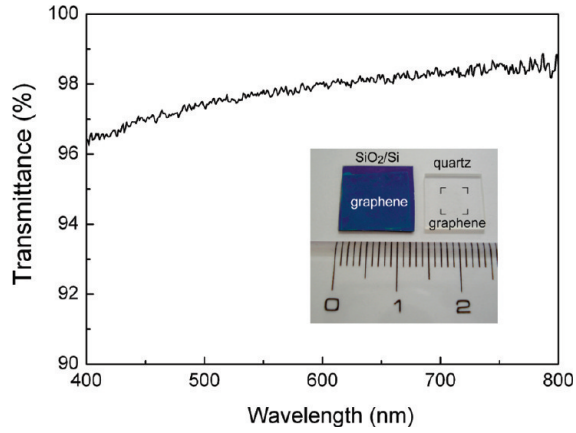

Figure 4. Optical transmittance of single-layer graphene transferred on a quartz substrate. Inset shows photograph of the graphene films transferred from the Co/c-plane sapphire to SiO_2(300 nm)/Si (left) and quartz (right) substrates.

Our estimation of the layer number based on the Raman spectra (I_{2D}/I_G ratio and line width of 2D band are used) may not be accurate enough to determine the precise layer number. This is because unintentional doping to graphene modifies the I_{2D}/I_G ratio,[25] which cannot be fully excluded in our growth and transfer processes. Also, double-layer graphene can have a relatively narrow line width of 30−40 cm^{-1}. Therefore, to confirm that the graphene film transferred from the Co/c-plane sapphire is single-layer, we measured light transmittance in the visible range. Shown in Figure 4 inset is a photograph of the graphene films transferred onto SiO_2/Si and quartz substrates. The graphene transferred on the SiO_2/Si shows a uniform film, indicating the transfer was done without deteriorating the graphene film due to a protecting poly(methyl methacrylate) (PMMA) layer. Using an optical-grade quartz substrate, we measured the light transmission through a hole with 1.8 mm diameter. As displayed in Figure 4, the graphene film showed the transmittance of 2.2 ± 0.2% at 550 nm, which is very close to the theoretical value of single-layer graphene (2.3%).[26,27] This result confirms that the transferred film consists of single-layer graphene.

Here, we discuss reasons for the growth of uniform single-layer graphene on the Co film crystallized on c-plane sapphire in spite of the high carbon solubility in Co at high temperature. It is reported that the precipitation of graphene occurs at grain boundaries of a metal catalyst.[19] In our crystalline Co film, the density of the grain boundaries is much lower than that of the polycrystalline Co film, as can be seen in Supporting Information, Figure SI-3 (Figure 3). Therefore, the graphene precipitation occurs more uniformly from limited sites when the appropriate amount of carbon is supplied. We note that the CH_4 concentration is essential for the uniform single-layer growth on our crystalline Co film; higher CH_4 concentration easily gives multilayer graphene. Thus, uniform and controlled

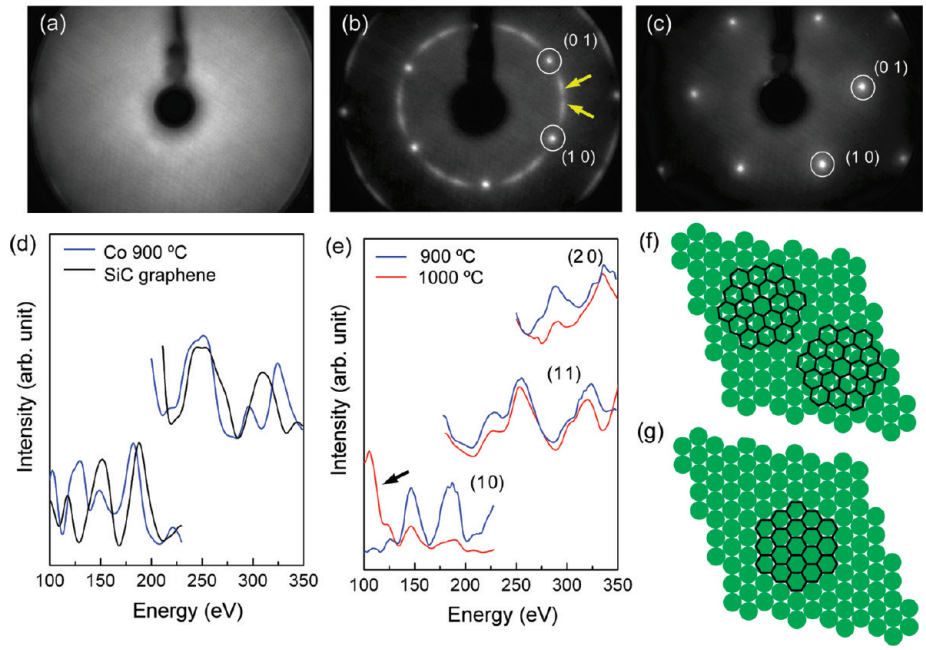

Figure 5. LEED patterns of Co/c-plane sapphire (a) and graphene/Co/c-plane sapphire grown at 900 °C (b) and 1000 °C (c). The beam energy is 180 eV. (d) *I*−*V* curve of the circular streaks highlighted by yellow arrows in panel b (blue curves). The data are compared with that obtained for graphene grown from SiC crystal (black curves).[28] (e) Comparison of intensity changes of (1 0), (1 1), and (2 0) diffraction spots for the samples grown at 900 and 1000 °C. Atomic models of orientation of graphene on the Co fcc(111) obtained for 900 °C (f) and 1000 °C (g) CVD samples.

graphitization as well as low density of grain boundaries is important for the uniform single-layer graphene growth.

We could also obtain single-layer graphene on the crystalline Co film at 900 °C, as shown in Supporting Information, Figure SI-6. In this case, few-layer graphene was partly observed. In the CVD at 900 °C, a higher concentration of CH_4 (~3%) was required to grow graphene than in the CVD at 1000 °C (~1%). Because of this higher CH_4 concentration, the precipitation is less controlled and gives thick graphene. It is also possible that the smaller domain size of graphene, as speculated from the Raman D band (Supporting Information, Figure SI-6b), increases the possibility of nucleation from many sites giving a more inhomogeneous graphene film.

Next, we investigated the orientation of graphene on the crystalline Co film. The epitaxy in graphene formation has been studied for single crystal surfaces, such as Ru(0001), Ir(111), and Ni (111), in surface science.[8−12] This is an ideal case because an ultrahigh vacuum system is used to expose atomically clean single crystal surfaces of metals. Note that the epitaxy has never been considered in the atmospheric CVD. In addition, these single crystal substrates are not practical for electronic applications because of the cost and limited size and, thus, the widely studied CVD deals with polycrystalline metal films. Therefore, we investigated the low-energy electron diffraction (LEED) for our atmospheric CVD-grown graphene to address the orientation of its hexagonal lattice. Shown in Figure 5 is LEED patterns measured in vacuum (below 8×10^{-9} Pa) at 80 K. When a Co film is subjected to H_2 annealing only (without supplying CH_4 for graphene growth), no clear LEED pattern was observed (Figure 5a), which indicates the absence of periodic surface structure. This can be explained by oxidation of the Co surface since the Co film was exposed to air during the transfer from the atmospheric CVD setup to the ultrahigh vacuum chamber. The Auger spectrum, shown in Supporting Information, Figure SI-7, indicates an intense O atom peak but no Co peak. Thus, the Co surface is heavily covered with O atoms so that no long-range order remains on the Co surface.

When graphene was grown at 900 °C, 6 sharp diffraction spots were observed together with 12 circular streaks (Figure 5b). Interestingly, this graphene/Co/c-plane sapphire sample showed a clear LEED pattern despite the sample being exposed to air after the CVD. We suppose that the graphene covers the Co film and prevents oxidation, thus maintaining the surface crystallinity of the Co film. Original LEED patterns with varied electron beam energies are displayed in Supporting Information, Figure SI-8. The six sharp spots can be assigned to the diffraction from the Co lattice, because these spots became stronger with increasing beam energy, which demonstrates the typical voltage dependence of transition metals. On the contrary, the 12 broad streaks, indicated by yellow arrows, became weaker with increasing beam energy. Figure 5d compares the intensity of these 12 broad streaks and that of diffraction spots measured for the graphene grown on SiC crystals.[28] The low energy peaks observed at 100−200 eV originate from graphene. Both samples

showed similar voltage dependence at 100−200 eV, proving that the 12 broad streaks originate in graphene formed on the crystalline Co film. These 12 broad streaks rotated from the Co spots by 22 ± 8°. This implies that graphene is rotated at 22 ± 8° with respect to the underneath Co lattice. The atomic model is illustrated in Figure 5f. Note that both Co hcp(0001) and fcc(111) have the same closest packing surface structure. As the beam size is about 1 mm, the model shows average orientation of the graphene.

When graphene was grown at a CVD temperature of 1000 °C, only six bright spots were detected without any circular streaks, as seen in Figure 5c. The *I*−*V* curves (Figure 5e) indicates that these six spots are coming from both Co lattice and graphene. At the high voltage (>200 eV) the diffraction mainly comes from the crystalline Co, while the diffraction from the as-grown graphene becomes dominant at the lower voltage (seen from the enhanced intensity at <150 eV indicated by the arrow). Therefore, we conclude that graphene grown at 1000 °C is epitaxially formed on the Co crystalline film, as illustrated in Figure 5g. Our results demonstrate that growing graphene over the crystalline Co film not only gives uniformity in the layer numbers, but also enables the control of the orientation of its hexagonal lattice. These findings are important when one tries to apply graphene for electronics.

There are several possible reasons for the observed mis-orientation in the graphene film grown at 900 °C (see Figure 5f). The first possible mechanism is attributed to the different thermal expansion coefficients of graphene and Co metal. Since graphene and Co lattice expand differently at high temperatures, it may change the graphene orientation with respect to the Co lattice at 900 and 1000 °C. Second, we speculate that C atoms adsorbed on the Co surface can migrate during CVD, and at higher temperature C atoms gains more thermal (or kinetic) energy. Thus, the higher temperature (1000 °C) results in the most stable orientation which matches with the Co fcc(111) lattice, while the lower temperature (900 °C) gives the substable orientation. Third, the degree of surface oxidation of the Co film is higher in the sample reacted at 900 °C than in that reacted at 1000 °C; the Auger spectra (Supporting Information, Figure SI-7) indicate that more O atoms and less Co atoms were present on the sample surface after the CVD at 900 °C when compared with that at 1000 °C CVD. This oxidized Co surface may cause surface reconstructuring, giving mis-orientation in the graphene film with respect to the Co lattice. It is unclear at the moment which mechanism is dominant, and *in situ* measurements are necessary to elucidate the mechanism. It is noted that the similar mis-orientation of single-layer graphene has been observed in the graphene grown on single crystalline Ir(111) and Pd(111) surfaces by ultra-high-vacuum (UHV) processes.[29,30]

Our epitaxial CVD growth approach is of great importance in the engineering of graphene films, because we can predict the graphene orientation from the crystallographic direction of the c-plane sapphire substrate. The armchair edge of graphene is supposed to be parallel to the [1 0 $\bar{1}$ 0] direction of c-plane sapphire. It is reported when metal nanoparticles deposited on a graphene film are annealed in H_2 the graphene is cut by the nanoparticles along crystallographic axes of graphene.[31,32] Supporting Information, Figure SI-9 demonstrates the cutting of our CVD-grown graphene. Most of the cutting lines are linear, suggesting high crystallinity of the CVD-grown graphene. This method is expected to be further developed to include the fabrication of graphene nanoribbons.

In conclusion, a highly crystalline Co film is realized on c-plane sapphire through high temperature sputtering and successive hydrogen annealing. Although it has been considered that selective growth of single-layer graphene over the transition metals with high carbon solubility such as Ni and Co is difficult, we can obtain uniform single-layer graphene over this crystalline Co film. The corresponding LEED pattern proves that single-layer graphene is epitaxially formed on this Co even by atmospheric CVD at 1000 °C; orientation of the graphene perfectly matches with the Co film underneath. This epitaxy makes it possible to predict the orientation of graphene. Our approach of the epitaxial CVD growth gives new insight on the growth mechanism of graphene and also provides a new means to grow single-layer graphene with controlled orientation over various crystalline metal films for high-performance electronic applications.

MATERIALS AND METHODS

Synthesis and Transfer of Graphene Film. Sapphire substrates (miscut angle <0.3°) were purchased from Kyocera Co; as-received substrates were used without intentional annealing process. The sapphire substrate has an atomically smooth surface, as inspected by AFM (surface roughness (root-mean-square (rms)) is 0.22 nm for 10 μm × 10 μm area); 200 nm thick Co films were deposited onto c-plane (0001) sapphire (α-Al_2O_3) and SiO_2(300 nm)/Si substrates with a power of 300 W in Ar atmosphere (0.6 Pa) by RF magnetron sputtering machine (Shibaura Mechatoronics Corp., CFS-4ES). Different substrate temperatures, room temperature, and 500 °C were employed during the sputtering. For CVD, the sample was loaded on a magnetic sample holder for the purpose of rapid cooling and then inserted into a horizontally set quartz tube. For the standard CVD procedure, the Co film was annealed in H_2 at 500 °C, followed by elevating the temperature to 1000 °C for catalytic pyrolysis of CH_4. After 20 min reaction, the sample was rapidly removed from the furnace in a protected gas flow of Ar and H_2. The detailed CVD condition is depicted in Supporting Information, Figure SI-1. For transfer of a graphene film onto a SiO_2/Si target substrate, we used PMMA and etching solution.[16] In brief, after the growth of graphene, the surface of graphene/Cu/substrate was covered with PMMA by spin-

coating. Thermal tape (Revalpha, Nitto-Denko) was attached onto the PMMA film. Then, the Co catalyst was dissolved with $FeCl_3$ aqueous solution to release the graphene supported with PMMA and thermal tape. Subsequently, the thermal tape/PMMA/graphene was washed with deionized water and transferred onto the SiO_2/Si substrate. Finally, the thermal tape was removed by heating at 120 °C, followed by PMMA removal with acetone.

Characterizations. Raman spectra and mapping images of graphene films were measured with a Jasco NRS-2100 instrument using 514.5 nm excitation wavelength. TEM images of samples prepared by a FIB (Hitachi NB 5000) were obtained with a Hitachi H-9500 at 300 keV acceleration voltage. SEM and AFM images were measured with a Hitachi S-4800 and a Nanoscope IIIa, respectively. The crystallinity of epitaxial Co film was measured by an XRD, (Riguku RINT 2500) and an SEM (Zeiss, Ultra55) equipped with an EBSD (TSL Solutions, OIM). Light transmission in the visible range was measured with UV−vis−NIR spectrometer (Jasco, V-570). The transmittance was measured through a circular hole with 1.8 mm diameter using a bare quartz substrate as reference. LEED patterns and Auger spectrum of as-grown graphene were recorded in an UHV chamber of $<8 \times 10^{-9}$ Pa with a Spectaleed (Omicron, Germany) instrument.

Acknowledgment. This work is supported by the PRESTO, Japan Science and Technology (JST), Grant-in-aid for Scientific Research from MEXT, and JSPS Funding Program for World-Leading Innovative R&D on Science and Technology (Development of Core Technologies for Green Nanoelectronics). TEM measurements were performed at Fukuryo Semiconductor Engineering, Co.

Supporting Information Available: CVD conditions, AFM images, EBSD data, CVD results of sapphire a- and r-planes, Raman spectrum taken before the transfer, the data obtained for 900 °C CVD, Auger spectra, other LEED patterns, and cutting image of the CVD graphene. This material is available free of charge *via* the Internet at http://pubs.acs.org.

REFERENCES AND NOTES

1. Geim, A. K.; Novoselov, K. S. The Rise of Graphene. *Nat. Mater.* **2007**, *6*, 183–191.
2. Bae, S.; Kim, H.; Lee, Y.; Xu, X.; Park, J. S.; Zheng, Y.; Balakrishnan, J.; Lei, T.; Kim, H. R.; Song, Y. I.; *et al.* Roll-to-Roll Production of 30-in. Graphene Films for Transparent Electrodes. *Nat. Nanotechnol.* **2010**, *5*, 574–578.
3. Lin, Y. M.; Dimitrakopoulos, C.; Jenkins, K. A.; Farmer, D. B.; Chiu, H. Y.; Grill, A.; Avouris, P. 100-GHz Transistors from Wafer-Scale Epitaxial Graphene. *Science* **2010**, *327*, 662.
4. De Arco, L. G.; Zhang, Y.; Schlenker, C. W.; Ryu, K.; Thompson, M. E.; Zhou, C. Continuous, Highly Flexible, and Transparent Graphene Films by Chemical Vapor Deposition for Organic Photovoltaics. *ACS Nano* **2010**, *4*, 2865–2873.
5. Li, S. L.; Miyazaki, H.; Kumatani, A.; Kanda, A.; Tsukagoshi, K. Low Operating Bias and Matched Input−Output Characteristics in Graphene Logic Inverters. *Nano Lett.* **2010**, *10*, 2357–2362.
6. Berger, C.; Song, Z.; Li, X.; Wu, X.; Brown, N.; Naud, C.; Mayou, D.; Li, T.; Hass, J.; Marchenkov, A. N.; *et al.* Electronic Confinement and Coherence in Patterned Epitaxial Graphene. *Science* **2006**, *312*, 1191–1196.
7. Rutter, G. M.; Crain, J. N.; Guisinger, N. P.; Li, T.; First, P. N.; Stroscio, J. A. Scattering and Interference in Epitaxial Graphene. *Science* **2007**, *317*, 219–222.
8. Usachov, D.; Dobrotvorskii, A. M.; Varykhalov, A.; Rader, O.; Gudat, W.; Shikin, A. M.; Adamchuk, V. K. Experimental and Theoretical Study of the Morphology of Commensurate and Incommensurate Graphene Layers on Ni Single-Crystal Surfaces. *Phys. Rev. B* **2008**, *78*, 85403−1-8.
9. Marchini, S.; Günther, S.; Wintterlin, J. Scanning Tunneling Microscopy of Graphene on Ru(0001). *Phys. Rev. B* **2007**, *76*, 75429−1-9.
10. Sutter, P. W.; Flege, J. I.; Sutter, E. A. Epitaxial Graphene on Ruthenium. *Nat. Mater.* **2008**, *7*, 406–411.
11. N'Diaye, A. T.; Bleikamp, S.; Feibelman, P. J.; Michely, T. Two-Dimensional Ir Cluster Lattice on a Graphene Moiré on Ir(111). *Phys. Rev. Lett.* **2006**, *97*, 215501−1-4.
12. Gamo, Y.; Nagashima, A.; Wakabayashi, M.; Terai, M.; Oshima, C. Atomic Structure of Monolayer Graphite Formed on Ni(111). *Surf. Sci.* **1997**, *374*, 61–64.
13. Yu, Q.; Lian, J.; Siriponglert, S.; Li, H.; Chen, Y. P.; Pei, S. S. Graphene Segregated on Ni Surfaces and Transferred to Insulators. *Appl. Phys. Lett.* **2008**, *93*, 113103−1-3.
14. Reina, A.; Jia, X.; Ho, J.; Nezich, D.; Son, H.; Bulovic, V.; Dresselhaus, M. S.; Kong, J. Large Area, Few-Layer Graphene Films on Arbitrary Substrates by Chemical Vapor Deposition. *Nano Lett.* **2009**, *9*, 30–35.
15. Arco, L. G. D.; Zhang, Y.; Kumar, A.; Zhou, C. Synthesis, Transfer, and Devices of Single- and Few-Layer Graphene by Chemical Vapor Deposition. *IEEE Trans. Nanotechnol.* **2009**, *8*, 135–138.
16. Kim, K. S.; Zhao, Y.; Jang, H.; Lee, S. H.; Kim, J. M.; Kim, K. S.; Ahn, J. H.; Kim, P.; Choi, J. Y.; Hong, B. H. Large-Scale Pattern Growth of Graphene Films for Stretchable Transparent Electrodes. *Nature* **2009**, *457*, 706–710.
17. Li, X.; Cai, W.; An, J.; Kim, S.; Nah, J.; Yang, D.; Piner, R.; Velamakanni, A.; Jung, I.; Tutuc, E.; *et al.* Large-Area Synthesis of High-Quality and Uniform Graphene Films on Copper Foils. *Science* **2009**, *324*, 1312–1314.
18. Massalski, T. B., Okamoto, H., Subramanian, P. R., Kacprzak, L. Eds. *Binary Alloy Phase Diagrams*, 2nd ed.; ASM International: Materials Park, OH, 1990.
19. Reina, A.; Thiele, S.; Jia, X.; Bhaviripudi, S.; Dresselhaus, M. S.; Schaefer, J. A.; Kong, J. Growth of Large-Area Single- and Bi-layer Graphene by Controlled Carbon Precipitation on Polycrystalline Ni Surfaces. *Nano Res.* **2009**, *2*, 509–516.
20. Bialas, H.; Heneka, K. Epitaxy of fcc Metals on Dielectric Substrates. *Vacuum* **1994**, *45*, 79–87.
21. Ago, H.; Tanaka, I.; Orofeo, C. M.; Tsuji, M.; Ikeda, K. Patterned Growth of Graphene over Epitaxial Catalyst. *Small* **2010**, *6*, 1226–1233.
22. Miyata, Y.; Kamon, K.; Ohashi, K.; Kitaura, R.; Yoshimura, M.; Shinohara, H. A Simple Alcohol-Chemical Vapor Deposition Synthesis of Single-Layer Graphenes Using Flash Cooling. *Appl. Phys. Lett.* **2010**, *96*, 263105−1-3.
23. Hansen, M., Ed. *Constitution of Binary Alloys*; McGraw-Hill: New York, 1958.
24. Giovannetti, G.; Khomyakov, P. A.; Brocks, G.; Karpan, V. M.; van den Brink, J.; Kelly, P. J. Doping Graphene with Metal Contacts. *Phys. Rev. Lett.* **2008**, *101*, 26803−1-4.
25. Casiraghi, C.; Pisana, S.; Novoselov, K. S.; Geim, A. K.; Ferrari, A. C. Raman Fingerprint of Charged Impurities in Graphene. *Appl. Phys. Lett.* **2007**, *91*, 233108−1-3.
26. Nair, R. R.; Blake, P.; Grigorenko, A. N.; Novoselov, K. S.; Booth, T. J.; Stauber, T.; Peres, N. M. R.; Geim, A. K. Fine Structure Constant Defines Visual Transparency of Graphene. *Science* **2008**, *320*, 1308.
27. Li, X.; Zhu, Y.; Cai, W.; Borysiak, M.; Han, B.; Chen, D.; Piner, R. D.; Colombo, L.; Ruoff, R. S. Transfer of Large-Area Graphene Films for High-Performance Transparent Conductive Electrodes. *Nano Lett.* **2009**, *9*, 4359–4363.
28. Hayashi, K.; Mizuno, S.; Tanaka, S. LEED Analysis of Graphite Films on Vicinal 6H-SiC(0001) Surface. *J. Novel Carbon Resource Sci.* **2010**, *2*, 17–20.
29. Loginova, E.; Nie, S.; Thürmer, K.; Bartelt, N. C.; McCarty, K. F. Defects of Graphene on Ir(111): Rotational Domains and Ridges. *Phys. Rev. B* **2009**, *80*, 85430−1-8.
30. Murata, Y.; Starodub, E.; Kappes, B. B; Ciobanu, C. V.; Bartelt, N. C.; McCarty, K. F.; Kodambaka, S. Orientation-Dependent Work Function of Graphene on Pd(111). *Appl. Phys. Lett.* **2010**, *97*, 143114−1-3.
31. Datta, S. S.; Strachan, D. R.; Khamis, S. M.; Johnson, A. T. C. Crystallographic Etching of Few-Layer Graphene. *Nano Lett.* **2008**, *8*, 1912–1915.
32. Campos, L. C.; Manfrinato, V. R.; Yamagishi, J. D. S.; Kong, J.; Herrero, P. J. Anisotropic Etching and Nanoribbon Formation in Single-Layer Graphene. *Nano Lett.* **2009**, *9*, 2600–2604.